SIDESWAY COLLAPSE OF A STEEL SPECIAL MOMENT FRAME SUBJECTED TO EARTHQUAKE LOADING

M. Del Carpio R.[1], G. Mosqueda [2], D. G. Lignos[3]

[1] Engineer, Structural Division, KPFF Consulting Engineers, Los Angeles, California, USA, maikol.delcarpio@kpff.com
(former Research Assistant at State University of New York at Buffalo, New York, USA)

[2] Associate Professor, Department of Structural Engineering, University of California, San Diego, California, USA, gmosqueda@eng.ucsd.edu

[3] Associate Professor, Department of Architecture, Civil and Environmental Engineering, Swiss Federal Institute of Technology, Lausanne (EPFL), Switzerland, dimitrios.lignos@epfl.ch

Abstract

Although a wealth of knowledge on the behavior of steel moment frame structures has been gained from past experimental studies, there are only a limited number of system-level tests examining seismic response near collapse. Such experimental data is essential to validate and improve analytical tools that generally rely on empirical and mechanical component-level models to capture the global system behavior. In view of the limited experimental data, a series of tests were conducted at the Network for Earthquake Engineering Simulation equipment site at the University at Buffalo. Hybrid simulation with substructuring was employed as a cost-effective alternative for large-scale system-level testing of large subassemblies. The ½-scale specimen, consisting of a 1½-bay by 1½-story subassembly, was designed to capture the behavior and interactions of beams, columns, panel zones, and the composite floor slab. The experimental setup permitted the application of lateral as well as varying vertical forces on the test specimen while maintaining realistic boundary conditions on the subassembly. This paper presents a description of the seismic performance of the different components of the tested subassembly.

Keywords: steel moment-resisting frames, seismic behavior, structural collapse, reduced beam sections, hybrid simulation

1. Introduction

An experimental program was conducted at the Network for Earthquake Engineering Simulation (NEES) equipment site at the University at Buffalo (UB) in response to the need highlighted by many researchers [1-3] for more realistic system-level experimental data for a comprehensive understanding of the seismic behavior of structures through collapse. In particular, very few past tests on steel moment-resisting frames (MRFs) provide sufficient and reliable information for deterioration modeling in support of collapse prediction under earthquake loading. Two notable full-scale tests on steel frame buildings with MRFs were conducted by Nakashima *et al*. [4] and Suita *et al*. [5]. However, shake table tests as discussed in the latter, have been limited due to financial constraints and the risk to personnel and equipment associated with collapsing structures. In this experimental program, hybrid simulation with substructuring is examined as a cost-efficient alternative to large-scale system-level testing of structures [6-9] and applied here to test a large subassembly of a steel MRF through collapse. In hybrid simulation, only key subassemblies are tested in the laboratory (i.e., physical substructures) while the rest of the structure is modeled analytically (i.e., numerical substructures), both interacting to simulate the response of the complete structural system. The test setup allows for the application of column axial forces from gravity loading as well as seismically-induced variations from dynamic overturning effects. A detailed description of the substructuring technique and integration method for these hybrid simulations is available in Del Carpio *et al*. [10, 11]. This paper presents a description of the seismic behavior of the steel MRF subassembly.

2. Experimental Program

A 4-story office building designed and evaluated by Lignos and Krawinkler [1] was selected as a prototype. The seismic force-resisting system consists of perimeter steel MRFs with reduced beam sections (RBS). This building was designed in Los Angeles, California according to U.S. codes/standards of practice [12-14]. Fig. 1 shows a schematic elevation of a ½-scale hybrid model developed to simulate the response of a MRF in the long direction of the prototype structure. Since moments and/or rotations at the boundaries are difficult to apply with linear hydraulic actuators, the following testing strategy was adopted. The physical substructure was extended to overlap with the numerical substructure (as shown by the dashed lines indicating the boundaries of both substructures) and its boundaries were simplified with hinges at mid-span of beams and columns. These simplifications were necessary to test this large subassembly using a reduced number of actuators available in a laboratory while maintaining the accuracy of the global response of the simulation. A detailed description of this strategy is available in Del Carpio *et al*. [11] and Hashemi and Mosqueda [9]. The numerical substructure was integrated with the physical substructure in the laboratory via OpenFresco [16]. Both physical and numerical components of the hybrid model were scaled in size by a length scale factor of S=0.50. During the hybrid simulations, the equations of motion were solved for the scaled model with the simulation time compressed by the time scale factor of $S^{1/2}$=0.707 based on similitude [17]. The wide-flange sections of the ½-scale model labeled in Fig. 1 were selected to match relevant target section geometric properties such as the moment of inertia (I_x), the cross-sectional area (A), the plastic modulus (Z_x), and local slenderness ratios ($b_f/2t_f$, h/t_w where b_f=flange width, t_f=flange thickness, h=distance between "k" areas within the web, and t_w=web thickness). Particularly, the local slenderness ratios are highly influential parameters to simulate cyclic deterioration in strength and stiffness of commonly used wide-flange sections [18].

The two-dimensional hybrid model was subjected sequentially to four increasing intensities of the 1989 Loma Prieta ground motion recorded at Los Gatos Presentation Center (LGPC), namely, 25% (elastic test), 100% (moderate yielding test), 150% (severe yielding test) and 200% (collapse test). The unscaled response spectra of this historical earthquake record matched approximately the spectra of the MCE assumed for the design of the prototype building.
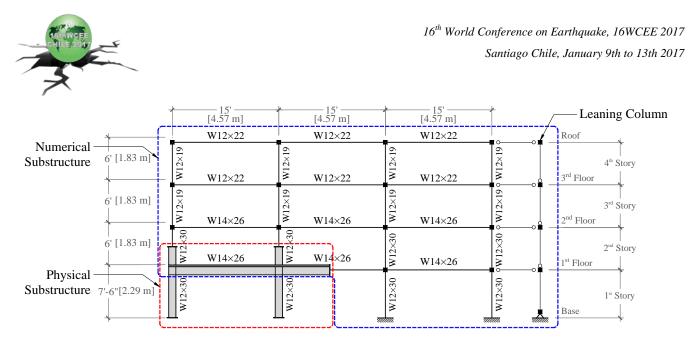
Fig. 1 – Schematic elevation of hybrid model of the steel MRF

2.1 Design and Construction of Test Specimen (Physical Substructure)

The test specimen was designed and constructed with several features of realistic moment frames including the floor slab. This consisted of light-weight concrete with a specified strength of 20 MPa (3000 psi) at 28 days and a maximum aggregate size of 13 mm (½ in) poured over a 20GA metal deck. The total thickness of the floor slab was 83 mm (3¼ in) where the depth of metal deck was 38 mm (1½ in) and the thickness of concrete slab was 44 mm (1¾ in). The concrete slab was reinforced with a 6×6-W1.4×W1.4 welded wire mesh placed over the entire floor area and reinforcing bars with a diameter of 9.5mm (#3 bars) across the girder for crack control due to gravity loading. Shear studs with a diameter of 10 mm ($^{3}/_{8}$ in) and a length of 64 mm (2½ in) were spaced at 152 mm (6 in) along the girder and floor beams (at each metal deck rib). The first shear stud was provided at 50 mm (2 in) away from the end of the RBS region to avoid the likelihood of fracture initiation. Although the prototype MRF was located along the perimeter of the building, the floor slab was constructed to extend out 610 mm (2 ft) to both sides of the girder to maintain symmetry and minimize any potential out-of-plane response during testing. The total width of the concrete slab matched the effective width per AISC [13] for an internal girder. While this physical model may not match the realism of a full composite floor system, it reasonably captures some of the slab effects including strengthening and stiffening of girders and panel zones. Details of the end RBS moment connection are shown in Fig. 2. The interior panel zone was reinforced with a 8 mm ($^{5}/_{16}$ in) thick doubler plate. The wide-flange sections and steel plates (continuity plates, shear-tab plates, doubler plates, etc.) were fabricated with A572 Grade 50 (i.e., F_y=345MPa) steel. The MRF column base connections consisted of 25 mm (1 in) thick base plates with 8 high-strength bolts (ASTM A325) of 25 mm (1 in) in diameter.

The test specimen was instrumented with 39 uniaxial strain gauges, 18 string displacements potentiometers (string pots), 4 linear potentiometers (linear pots) and 27 light-emitting diodes (LEDs) part of the Krypton coordinate tracking system. The Krypton system tracks the three-dimensional position of LEDs with a system of infrared cameras. Distribution of bending moments and axial forces on the moment frame was derived from strain gauge measurements. String pot and LED measurements were used to approximate rotations over plastic-hinge regions in columns and girders. Panel zone distortions were measured with V-shaped arrangements of linear pots at each beam-to-column joint. The tracking system was also used to approximate rotations of the end column base plate. A detailed description of the instrumentation system including instrumentation drawings is available in Del Carpio *et al*. [10].

2.2 Numerical Substructure Model

The numerical substructure was modeled in OpenSees [15] using a concentrated plasticity approach. The hysteretic model developed by Ibarra *et al*. [19] and modified by Lignos and Krawinkler [1] was assigned to rotational spring elements simulating the inelastic flexural response at plastic-hinge zones of girders and

columns of the MRF. This model was previously calibrated by the latter researchers [20] using an extensive database of over 300 structural W-section components, primarily beams but also very few columns. In addition, some of the effects of the composite floor slab on the response of the girders such as the asymmetric hysteretic behavior as well as girder stiffening were accounted for based on past studies [21-25]. This model does not account for cyclic hardening. However, the effect of isotropic hardening was accounted for by increasing the predicted yield bending strength $M_{y,p}$ (plastic section modulus times the measured yield strength) to an effective value M_y. This one-dimensional hysteretic model does not account for axial force-bending moment (P-M) interaction as currently implemented in OpenSees. However, this is a reasonable assumption to simulate the response of columns in low-rise structures with low levels of column axial forces as demonstrated by recent small- and full-scale collapse tests [5, 18, 26]. The joints of the moment frame were simulated using a panel zone model [27] to account for joint deformation. Geometric nonlinearities were simulated with the simplified P-Delta formulation in OpenSees. P-Delta effects from the remaining weight of the building (weight not modeled in the MRF) were carried by a leaning column included in the numerical model. Flexible supports were included to match the experimentally-measured column base flexibility of the test specimen. The modified Rayleigh damping by Zareian and Medina [28] was employed to overcome some of the limitations of the classical Rayleigh damping associated with unrealistic damping forces that can influence the collapse capacity of a system. Two percent inherent damping was assigned to the first two natural frequencies of the steel MRF.
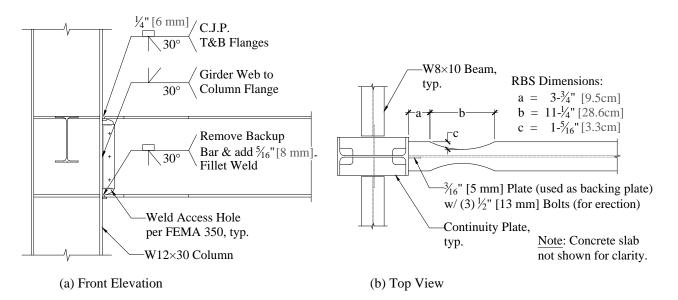

Fig. 2 – Details of end RBS moment connection

2.3 Experimental Test Setup

The experimental test setup shown in Fig. 3 was designed to apply lateral as well as vertical loads on the test specimen. Clevises were conveniently provided at the top of the columns of the test specimen to simplify its boundary conditions. As previously mentioned, these simplified boundary conditions were handled by the substructuring strategy discussed in Del Carpio *et al.* [11]. The test specimen was mounted on the strong floor using two interface 274.3×152.4×3.8 cm (9'×5'×1½") steel plates. These were sufficiently strong to allow for the development of the full plastic moment within the column but added some flexibility at the column supports. A frame surrounded the test specimen and provided out-of-plane support. The girder of the test specimen in cantilever was underpinned with a vertical link member to limit vertical deflection at the tip and generate a moment at the column connection. The various components of the test setup (support frame, reaction frame, and horizontal and vertical link members) were connected through clevises so that, under the application of lateral

loads, the supporting frame swayed as shown in Fig. 3 and guided the test specimen in the direction of loading providing minimal lateral resistance.

Lateral loading was applied with two horizontal actuators controlling the lateral displacements at the first and mid-second story levels of the test specimen. The horizontal link member transferred lateral loads from the top horizontal actuator to the top of the test specimen columns connected by pins. The bottom horizontal actuator was connected to the first floor of the test specimen. This load path is somewhat different to that of a realistic MRF where the floor inertial forces are transferred via collector beams. Gravity loads on the first floor were simulated using steel plates. Two 37.8-kN (8.5-kip) steel plates accounted for a total uniformly distributed dead load of 4.3 kPa [90 pound per square foot (psf)] and 25% of the code-specified live load of 2.4 kPa (50 psf). Additional gravity loads on the columns of the test specimen from upper stories as well as earthquake-induced variations from dynamic overturning forces were applied with two vertical actuators. A reaction frame for these actuators was mounted on top of the support frame as shown in Fig. 3. A vertical guide connection was devised between the reaction frame and horizontal link member. It consisted of a vertical steel pipe (connected to the horizontal link member at the bottom) freely sliding inside an outer pipe (connected to the reaction frame at the top and braced to maintain a right angle). This connection provided horizontal coupling between the reaction frame and the horizontal link member without transferring vertical forces. This helped to maintain a vertical alignment of the force-controlled actuators (mounted between these two members) and to accommodate the actuator vertical displacements.
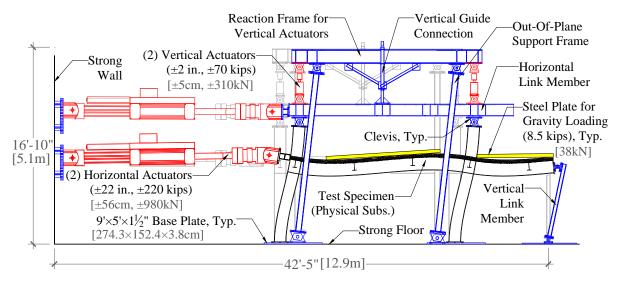

Fig. 3 – Experimental test setup for hybrid simulation at UB-NEES Site

3. Test Results and Seismic Behavior of Steel Special MRF

Table 1 summarizes peak roof drifts (ratio of roof lateral deformation to height of building from base to roof), peak first-story drifts (ratio of first floor lateral deformation to height from base to first floor) and peak plastic rotations at plastic-hinge regions within beams and columns for each test. The moment frame remained elastic during the first test HS01-25%. Flexural yielding within the RBS regions and column bases as well as limited panel zone yielding initiated during HS01-100%. These energy dissipation and plastic mechanisms are in agreement with the strong-column-weak-beam design criterion in current seismic code provisions for steel MRFs. Upon further loading, the flexural strength of steel beams and columns deteriorated due to local buckling during the HS01-160% test. Dynamic instability of the moment frame occurred during the last test HS01-200% where second-order P-Delta effects fully exceeded the shear resistance of the structure and therefore accelerated a sidesway plastic mechanism formed over the lower three stories (i.e., structural collapse). The test was terminated when a stroke of 508 mm (20 in) was reached at the top horizontal actuator, corresponding to a

16.4% first-story drift and a 10.6% roof drift. Prior to the test, fully numerical predictions indicated that sidesway collapse of the frame structure was imminent at this level of deformation. Lateral-torsional buckling of the girders occurred toward the end of the test which caused column yielding in out-of-plane bending, particularly in the interior column. This is a deficiency of the test setup which did not properly restrain lateral-torsional bucking. While this could affect the outcome of the results, such as the unloading stiffness of girders and columns, twisting of the girder occurred only at the very end of the hybrid simulations. Out-of-plane bending was less pronounced in the end column due to the connection of the horizontal actuator which provided torsional restraint. These observations are consistent with past experiments with RBS beam-to-column connections [30, 31]. A detailed description of the seismic behavior of the different components of the test specimen is provided below.

Table 1 – Selected test results of sequential hybrid simulations through collapse

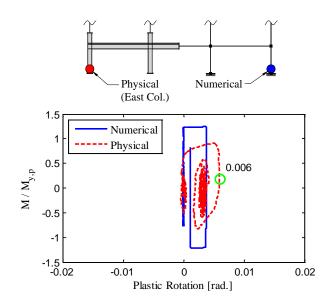| Test ID | Roof Drift [%] | First-Story Drift [%] | Peak Rotation of Plastic-Hinge Regions in Test Specimen [rad] | | | | | | |
			End Column		Interior Column		Girder*		
			Base	Top	Base	Top	A	B	C
HS01-25%	−0.7	−0.8	0.000	0.000	0.000	0.000	0.000	0.000	0.000
HS01-100%	−1.7	−2.3	0.006	0.000	0.003	0.000	−0.006	+0.005	−0.003
HS01-160%	−5.9	−7.6	0.067	0.003	0.039	0.017	−0.074	+0.043	−0.037
HS01-200%	−10.6	−16.4	0.165	0.025	0.146	0.101	−0.161	+0.111	−0.078

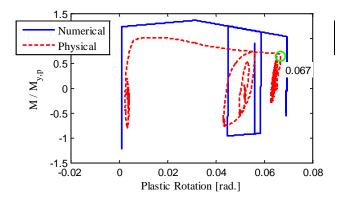* See Fig. 5(a) for girder plastic-hinge locations A, B and C.

3.1 Steel Columns

Consistent with the plastic sidesway mechanism of the moment frame, damage on columns was concentrated mainly at the base (i.e., near the supports). Asymmetric column yielding (yielding in one direction) started during the HS01-100% test as seen in the deduced moment-rotation plots in Fig. 4(a) for the end column. Bending moments were derived from strain gauge measurements. The response of a similar numerical model, provided for comparison, indicates that the yield strength was over-predicted. This was mainly due to the increase of the predicted yield bending moment $M_{y,p}$ by a factor of 1.17 to account for the effect of isotropic hardening in the numerical component. To a lesser extent, this could be attributed to the hysteretic model, which did not account for axial force-bending moment (P-M) interaction. Plastic P-M interactions diagrams indicate less than a 5% reduction in the column bending capacity for the maximum levels of axial load. During this test, the end column experienced the largest axial force variations due to dynamic overturning moments from $0.17P_{y,p}$ in compression to $0.10P_{y,p}$ in tension ($P_{y,p}$=column cross-sectional area times the measured material yield). The interior column remained in compression exhibiting smaller variations from $0.07P_{y,p}$ to $0.10P_{y,p}$. A photograph of the end column is presented in Fig. 4(b). The darker regions in the column, where the whitewash paint (mixture of lime and water) cracked and peeled, indicate yielding and/or local buckling. Upon further loading during the HS01-160% test, plastic hinges fully formed at the column bases and experienced large levels of inelastic deformation as seen in Fig. 4(c). The web and flange in compression of the end column in particular exhibited local buckling as seen in Fig. 4(d). This results in strength and stiffness deterioration of the column as observed by the negative slope in the moment-rotation relation. Local buckling at column bases shifted the inflection point in the columns towards their mid-height and resulted into larger flexural demands at the top of the first-story columns. This is typical in steel MRFs due to the column base flexibility [29] and became more evident near collapse. Deterioration accelerated during the last test HS01-200% as shown in Fig. 4(e) leading to structural collapse of the MRF. The numerical substructure over-predicted strength deterioration as measured by the post-capping plastic rotation (defined as difference between rotation at complete loss of flexural strength and rotation at maximum moment) of the W12×30 column. This was expected since the predictive equations of Lignos and Krawinkler for deterioration parameters were derived with an experimental database of mostly W21 sections and above. Smaller sections such as the W12×30 tested here typically exhibit larger plastic rotation capacities because of their dependence on depth [20]. The post-capping plastic rotation is one of the most influential parameters [32] in collapse assessment of structural systems. As previously indicated, lateral-torsional buckling
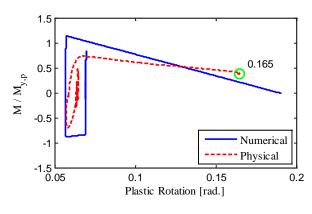
of the girders towards the end of the test induced yielding at the top of the first-story columns in out-of-plane bending. Similar observations were made in prior experimental work on beam-to-column subassemblies that utilized RBS connections [30, 31].

(a) Moment-rotation plot, Test ID: HS01-100%

(b) Photograph, Test ID: HS01-100%

(c) Moment-rotation plot, Test ID: HS01-160%

(d) Photograph, Test ID: HS01-160%

(e) Moment-rotation plot, Test ID: HS01-200%

(f) Photograph, Test ID: HS01-200%

Fig. 4 – Deduced moment-rotation relations for end column and photographs of damage state
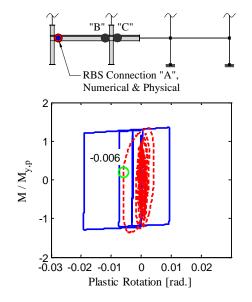
3.2 Girders with RBS

Bending moments in girders were derived similarly to those in columns but the estimates are of a more approximate nature due to the presence of the concrete slab. These approximate bending moments are carefully assessed to make observations and draw conclusions. As in the case of columns, the formation of plastic hinges within the RBS regions initiated during the first inelastic test HS01-100% exhibiting minor symmetric yielding (yielding in both directions) as seen in Fig. 5(a) for the end RBS location (location "A"). Since the neutral axis is closer to the top flange due to the presence of the floor slab, yielding as indicated by whitewash peeling in Fig. 5(b) occurred near the bottom flange. Local buckling initiated during the HS01-160% test. As indicated before, local buckling causes strength and stiffness deterioration of the girder as observed in the moment-rotation response of the girder near the end RBS in Fig. 5(c). A photograph of the deteriorated girder is shown in Fig. 5(d). Practically negligible local buckling of the top flanges of the beams is observed due to the presence of the floor slab. The bottom flange was more susceptible to local buckling. Due to the frame continuity, local buckling of the bottom flanges in the RBS region was not severe. This agrees from observations on composite connections as summarized in Elkady and Lignos [22]. Web local buckling was the primary contributor to flexural strength deterioration of the girders with RBS as summarized from previous tests in Lignos and Krawinkler [20]. Recognizing the lesser accuracy of the derived bending moments in girders as compared to those in columns, the yield strength of the girder with RBS appears to be reasonably predicted in the numerical substructure. Fig. 5(e) shows the response of the same plastic hinge near collapse (HS01-200% test). Lateral-torsional buckling of the girder occurred toward the end of the simulation. The twisting of the girder has been observed in prior sub-assemblage tests conducted by Chi and Uang [30] and Zhang and Ricles [31]. This is a deficiency of the test setup which did not prevent torsion of the girder and floor slab. Strength deterioration of this particular W14×26 girder with RBS also appears to be slightly under-predicted in the numerical portion of the hybrid model.
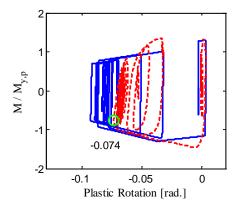
3.3 Panel Zone

Panel zone distortions are faithfully measured using the Krypton system. However, malfunctioning and deficient installation of the linear pots on the interior panel zone precluded the collection of data for this joint. During the elastic test HS01-25%, the end panel zone was approximately 30% stiffer than its corresponding numerical counterpart, which did not account for the effects of the floor slab on the panel zone hysteretic behavior. This observation is consistent with prior studies [22, 33]. The largest inelastic response of the panel zones occurred during the first inelastic test HS01-100% observed in Fig. 6(a). The flexural strength of the girders and columns deteriorated with the progression of inelastic cycles in subsequent tests and consequently induced smaller stresses to the panel zones. The moments are the sum of column bending moments above and below the panel zone normalized by the predicted panel zone yield moment strength ($M_{y,p}$=0.55F_y d_c t d_b where F_y=measured material yield strength, d_c=column depth, t=panel zone thickness, d_b=girder depth). Due to concrete slab cracking, the unloading stiffness of the panel zone deteriorated during this test and became similar to the theoretical stiffness of the bare panel zone in the numerical component. Though to a lesser extent, panel zone yielding was still observed during the HS01-160% test. The predicted shear capacity according to the Krawinkler equations [34] was fairly close to the observed yield shear resistance of both panel zones. This is to be expected for this size of cross sections with thin webs as discussed in Krawinkler and Mohasseb [35]. The Krawinkler [34] model over-predicts the panel zone shear strength in the negative loading direction. This finding is in line with earlier analytical studies [36-38] related to the hysteretic response of the beam-to-column panel zone joint as part of steel MRFs. Interestingly, in the positive loading direction (i.e., slab in compression), the panel zone model predicts reasonably well the panel zone yield moment even though its shear strength was not adjusted due to the presence of the floor slab [22]. It should be stated that the Krawinkler model does not explicitly capture isotropic hardening. The predicted panel zone shear strength is only adjusted to inherently consider this effect. However, depending on the steel material the effects of the isotropic hardening on the panel zone hysteretic response may be significant as suggested by a number of subassembly experiments that were conducted as part of the SAC program [39]. For the same reasons, the inelastic range of the panel zone shear distortion is under-predicted compared to what was measured during the hybrid simulation experiments. The response of the exterior panel zone during the collapse test HS01-200% was practically elastic since the strength of girders and columns significantly deteriorated.
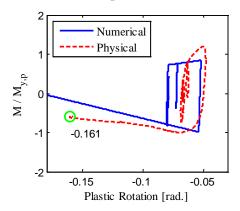
(a) Moment-rotation plot, Test ID: HS01-100%

(b) Photograph, Test ID: HS01-100%

(c) Moment-rotation plot, Test ID: HS01-160%

(d) Photograph, Test ID: HS01-160%

(e) Moment-rotation plot, Test ID: HS01-200%
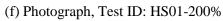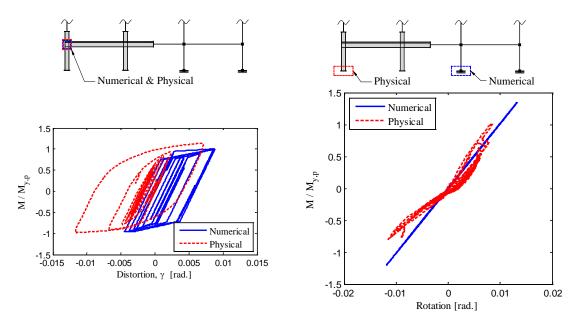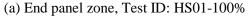
(f) Photograph, Test ID: HS01-200%

Fig. 5 – Deduced moment-rotation relations for girder and photographs of damage state

3.4 Column Base Plates

The response of the end column base plate as depicted with plots of bending moments at the base of the column versus rotations of the base plate (obtained with LEDs) exhibited a fairly linear response from the elastic test through that near collapse. Fig. 4(b) shows the response during the HS01-160% test. This indicates an elastic response of base plate, anchor bolts and interface steel plates between the test specimen and the strong floor in the laboratory. The elastic stiffness of this response shows almost no deterioration upon cyclic loading and closely matched that of the numerical model.

(a) End panel zone, Test ID: HS01-100%   (b) End base plate, Test ID: HS01-160%

Fig. 6 – Force-deformation relationships for end panel zone and base plate

3.5 Response of Concrete Slab

Damage of the concrete floor slab of the test specimen was limited to the region around the columns. Some concrete spalling was observed around the interior column.

5. Summary and Conclusions

A 1½-bay by 1½-story subassembly of a steel MRF with floor slab was tested via hybrid simulation from the onset of damage through incipient collapse. This large subassembly allowed for key observations of component behavior (girder, column, panel zones, column base plates, etc.), and their connections and interactions with neighboring members under realistic combinations of lateral and vertical loads. These tests thus represent an improvement to traditional component-level tests on cruciform or T-shaped subassemblies. The observed behavior of the frame structure with damage distributed throughout the various components highlights the benefits of the hybrid test approach with large subassemblies towards a better understanding of component interaction and system-level behavior prior to collapse.

4. Acknowledgements

gratefully acknowledged. Any opinions, findings, and conclusion or recommendation expressed in this paper are those of the authors and do not necessarily reflect the views of the sponsor. The authors thank the laboratory personnel at University at Buffalo for their technical support and guidance during the design and construction of the experimental setup.

5. References

[1] Lignos, D. G., and Krawinkler, H. (2012): "Sidesway Collapse of Deteriorating Structural Systems under Seismic Excitations." Rep. No. TB 172, The John A. Blume Earthquake Engineering Research Center, Stanford University, CA.

[2] Nakashima, M. (2008): "Roles of large structural testing for the advancement of earthquake engineering." Proc., 14th World Conf. Earthquake Eng., Beijing.

[3] Villaverde, R. (2007): "Methods to Assess the Seismic Collapse Capacity of Building Structures: State of the Art." J. Struct. Eng., 133(1), 57-66.

[4] Nakashima, M., Matsumiya, T., Suita, K., and Liu, D. (2006): "Test on Full-Scale Three-Storey Steel Moment Frame and Assessment of Ability of Numerical Simulation to Trace Cyclic Inelastic Behaviour." Earthquake Engng. Struct. Dyn., 35(1), 3-19.

[5] Suita, K., Yamada, S., Tada, M., Kasai, K., Matsuoka, Y., and Shimada, Y. (2008): "Collapse Experiment on Four-Story Steel Moment Frame: Part 2". Proc. 14th World Conf. Earthquake Eng., Beijing, China.

[6] Mahmoud, H., Elnashai, A., Spencer, B., Jr., Kwon, O., and Bennier, D. (2013): "Hybrid Simulation for Earthquake Response of Semirigid Partial-Strength Steel Frames." J. Struct. Eng., 139, Special Issue: NEES 1: Advances in Earthquake Eng., 1134-1148.

[7] Schellenberg, A. H., Huang, Y., and Mahin, S. A. (2008): "Structural FE-Software Coupling through the Experimental Software Framework, OpenFresco." Proc. 14th World Conf. Earthquake Eng., Beijing, China.

[8] Wang, T., Mosqueda, G., Jacobsen, A., and Delgado, M. C. (2012): "Performance Evaluation of a Distributed Hybrid Test Framework to Reproduce the Collapse Behaviour of a Structure." J. Earthquake Eng. Struct. Dyn., 41(2), 295-313.

[9] Hashemi, M. J., and Mosqueda, G. (2014): "Innovative Substructuring Technique for Hybrid Simulation of Multi-Story Building through Collapse." Earthquake Eng. Struct. Dyn., 43(14), 2059-2074.

[10] Del Carpio R., M., Mosqueda, G., and Lignos, D. G. (2014): "Hybrid Simulation of the Seismic Response of a Steel Moment Frame Building Structure through Collapse." Technical Report MCEER-14-0003, State University of New York at Buffalo, NY.

[11] Del Carpio R., M., Mosqueda, G., and Hashemi, M. J. (2015): "Large-Scale Hybrid Simulation of a Steel Moment Frame Building Structure through Collapse." J. Struct. Eng., DOI: 10.1061/(ASCE)ST.1943-541X.0001328.

[12] International Building Code (IBC) (2003): International Code Council, Birmingham, AL.

[13] American Institute of Steel Construction (AISC) (2010): Seismic Provisions for Structural Steel Buildings, including Supplement No. 1, Chicago.

[14] American Society of Civil Engineers (ASCE). (2002): Minimum Design Loads for Buildings and Other Structures (SEI/ASCE-02), Virginia.

[15] McKenna, F., Fenves, G. L., Scott, M. H. (2000): Open system for earthquake engineering simulation (OpenSees). University of California, Berkeley, CA.

[16] Open Framework for Experimental Setup and Control (OpenFresco). (2008): Pacific Earthquake Engineering Research Center (PEER), (http://openfresco.berkeley.edu).

[17] Moncarz, P. D., and Krawinkler, H. (1981): "Theory and Application of Experimental Model Analysis in Earthquake Engineering." Rep. No. 50, The John A. Blume Earthquake Engineering Research Center; Stanford University, CA.

[18] Lignos, D. G., Krawinkler, H., and Whittaker, A. S. (2011): "Prediction and validation of sidesway collapse of two scale models of a 4-story steel moment frame." Earthquake Eng. Struct. Dyn., 40(7), 807-825.

[19] Ibarra, L. F., Medina, R. A., and Krawinkler, H. (2005): "Hysteretic Models that Incorporate Strength and Stiffness Deterioration." Earthquake Eng. Struct. Dyn., 34(12), 1489-1511.

[20] Lignos, D. G., and Krawinkler, H. (2011): "Deterioration Modeling of Steel Components in Support of Collapse Prediction of Steel Moment Frames under Earthquake Loading." J. Struct. Eng. 137(11), 1291-1302.

[21] Lignos, D., Eads, L., and Krawinkler, H. (2011): "Effect of Composite Action on Collapse Capacity of Steel Moment Frames under Earthquake Loading." EUROSTEEL, Budapest, Hungary.

[22] Elkady A., and Lignos, D. G. (2014): "Modeling of the composite action in fully restrained beam-to-column connections: implications in the seismic design and collapse capacity of steel special moment frames." Earthquake Eng. Struct. Dyn., 43(13), 1935-1954.

[23] Leon, R., Hajjar, J., and Gustafson, M. (1998): "Seismic Response of Composite Moment-Resisting Connections. I: Performance." J. Struct. Eng., 124(8), 868-876.

[24] Nam, T. T. and Kasai, K. (2012): "Study on Shake Table Experimental Results regarding Composite Action of a Full-Scale Steel Building tested to Collapse." 9th Int. Conf. on Urban Earthquake Eng./4th Asia Conf. on Earthquake Eng., Tokyo, Japan.

[25] Lee, S. and Lu, L. (1989): "Cyclic Tests of Full-Scale Composite Joint Subassemblages." J. Struct. Eng., 115(8), 1977-1998.

[26] Lignos, D. G., Hikino, T., Matsuoka, Y., and Nakashima, M. (2013): "Collapse Assessment of Steel Moment Frames Based on E-Defense Full-Scale Shake Table Collapse Tests." J. Struct. Eng., 139(1), 120-132.

[27] Federal Emergency Management Agency (FEMA). (2000): State of the Art Report on Performance Prediction and Evaluation of Steel Moment-Frame Buildings (FEMA 355F), Washintong, D.C.

[28] Zareian, F., and Medina, R. A. (2010): "A Practical Method for Proper Modeling of Structural Damping in Inelastic Plane Structural Systems." Computers and Structures, 88(1-2), 45-53.

[29] Zareian, F., Kanvinde, A. (2013): "Effect of Column-Base Flexibility on the Seismic Response and Safety of Steel Moment-Resisting Frames", Earthquake Spectra, 29(4):1537-59.

[30] Chi, B. and Uang, C. (2002): "Cyclic Response and Design Recommendations of Reduced Beam Section Moment Connections with Deep Columns." J. Struct. Eng. 128, SPECIAL ISSUE: STEEL MOMENT FRAMES AFTER NORTHRIDGE—PART II, 464–473.

[31] Zhang, X., and Ricles, J. (2006): "Experimental Evaluation of Reduced Beam Section Connections to Deep Columns." J. Struct. Eng., 132(3), 346-357.

[32] Ibarra, L. F., and Krawinkler, H. (2005): "Global Collapse of Frame Structures under Seismic Excitations." Rep. No. PEER 2005/06, Univ. of California, Berkeley, CA.

[33] Kim, K. D., and Engelhardt, M. D. (2002): "Monotonic and Cyclic Loading Models for Panel Zones in Steel Moment Frames." Journal of Constructional Steel Research, 58(5-8), 605-635.

[34] Krawinkler, H. (1978): "Shear in Beam-Column Joints in Seismic Design of Steel Frames." Engineering Journal, American Institute of Steel Construction, 5(3), 82-91.

[35] Krawinkler, H. and Mohasseb, S. (1987): "Effects of Panel Zone Deformations on Seismic Response." Journal of Constructional Steel Research, Vol. 8, pp. 233-250.

[36] Charney, F.A. and Downs, W.M. (2004): "Modeling Procedures for Panel Zone Deformations in Moment Resisting Frames," Proceedings, Connections in Steel Structures V, Amsterdam, Netherlands.

[37] Kim, K.D. and Engelhardt, M.D. (2002): "Monotonic and cyclic loading models for panel zones in steel moment frames," Journal of Constructional Steel Research, 58, 605-635.

[38] Wang, S.J., 1988, Seismic Response of Steel Building Frames with Inelastic Joint Deformation, Ph.D. Dissertation, Department of Civil Engineering, Lehigh University, Bethlehem, Pennsylvania.

[39] Federal Emergency Management Agency (FEMA). (2000): State of the Art Report on Connection Performance (FEMA 355D), Washington, D.C.